Indicators of abnormal PET coronary flow capacity in detecting cardiac ischemia

Andrew Van Tosh[1] · Omar Khalique[1] · C. David Cooke[2] · Christopher J. Palestro[3] · Kenneth J. Nichols[3]

Abstract
Coronary flow capacity (CFC) categorizes severity of left ventricular (LV) ischemia by PET myocardial blood flow (MBF). Our objective was to correlate abnormal CFC with other indicators of regional ischemia. Data were examined retrospectively for 231 patients evaluated for known/suspected CAD who underwent rest and regadenoson-stress ^{82}Rb PET/CT. MBF and myocardial flow reserve (MFR) were quantified, from which CFC was categorized as Normal CFC (1), Minimally reduced (2), Mildly reduced (3), Moderately reduced (4), and Severely reduced (5) for the three main arterial territories as well as globally. Relative perfusion summed stress score (SSS) and systolic phase contraction bandwidth (BW) were assessed. Accuracy to detect arteries with CFC ≥ 4 was highest for a Regional Index combining SSS and BW ($88 \pm 3\%$). A Global Index formed from stress ejection fraction, SSS and BW was the most accurate means of identifying patients with global CFC ≥ 4 ($84 \pm 3\%$). Arteries with abnormal CFC derived from absolute myocardial blood flow measurements are accurately identified by composite parameters combining regionally aberrant relative perfusion patterns and asynchrony.

Keywords Ischemia · PET · Rb-82 · Coronary flow capacity

Introduction

PET/CT myocardial perfusion imaging is a powerful means of assessing CAD and can detect abnormal perfusion by comparing relative tracer uptake to a normal database [1], or quantifying absolute rest and stress left ventricular (LV) myocardial blood flow (MBF) [2]. PET/CT may have advantages over conventional angiography, qualitative interpretation of which can be variable [3, 4]. PET/CT may detect abnormally reduced MBF and regional wall motion abnormalities in patients with jeopardized myocardium whose arterial stenosis appear < 70% on catheterization [5].

Myocardial flow reserve (MFR = stress MBF/rest MBF) is calculated regionally for each coronary territory, and globally [6]. Global MFR can define groups at risk for major adverse cardiac events (MACE) [7]. Regional MFR values < 1.6 identifies coronary distributions likely to be supplied by a vessel with a hemodynamically significant epicardial stenosis [3]. For assessing cardiac disease, both global and regional approaches to MBF have been used [8, 9]. An alternative system for categorizing regional MBF and myocardial ischemia is coronary flow capacity (CFC) based on ischemic thresholds [10], ranging from normal stress MBF and MFR to severe reductions in both parameters. This approach has been used to classify arterial territories by mean stress MBF and MFR values using ^{82}Rb [11], ^{13}N–H$_3$ [12], and ^{15}O–H$_2$O [13]. Patients with coronary territories showing severe CFC impairment are at increased risk for MACE [9]. MBF can be improved, and risk mitigated with re-vascularization [9, 11]. Whether provocable ischemia exists at lower levels of CFC is not fully established.

Recently, PET evaluation of coronaries with angiographically borderline stenosis demonstrated that stress-induced worsening of complex measures of LV asynchrony could serve as early evidence of stenoses being hemodynamically significant [14]. Other investigators have documented increased incidence of death and MACE's in patients with non-obstructive CAD for whom territorial CFC was abnormal [12]. In this study, we analyzed ^{82}Rb regadenoson PET/

✉ Kenneth J. Nichols
Knichols@Northwell.edu

1 St. Francis Hospital, Roslyn, NY, USA

2 Department of Radiology, Emory University, Atlanta, GA, USA

3 Department of Radiology, Donald and Barbara Zucker School of Medicine at Hofstra/Northwell, Hempstead, NY, USA

CT studies to identify an index combining relative perfusion, wall motion and asynchrony parameters which best separated CFC categories. We compared global parameters to global CFC values, and regional parameters to regional CFC values. We established the normal range of values for the regional index in coronaries with no hemodynamic obstruction, using coronary arteriography to identify definitely unobstructed arteries. We hypothesized that evidence of ischemia is manifested as abnormal values of this index not only in the most severe classes of CFC [9, 11], but also in patients with less severe impairment of MBF and MFR.

Methods

Patients

We retrospectively analyzed data of 231 patients who had [82]Rb rest and regadenoson-stress PET/CT scans for known or suspected CAD (age 69 ± 13 years; 94 female patients; 137 male patients). 58 (25%) patients had PCI, 52 (23%) had MI's and 41 (18%) had CABG, 105 of whom also had quantitative coronary angiography (age 69 ± 13 years; 42 females; 63 males). Time between PET and angiography was 138 ± 388 days, with no intervening cardiac events (e.g., PCI or MI). Of these 105 patients, 39% patients had PCI, 22% had MI and 24% had CABG. We studied this subgroup to define normal ranges of LV functional and perfusion parameters in arterial territories with no significant obstructive CAD.

The Institutional Review Board approved this retrospective study and the requirement to obtain informed consent was waived. All data were handled in compliance with the Health Insurance Portability and Accountability Act of 1996.

PET data collection

PET/CT studies were acquired in gated list mode on a GE Discovery VCT 64 PET/CT in 2D mode or on a GE D710 PET/CT 64-slice CT system in 3D mode following standard published guidelines [15, 16]. A bolus of 0.94–1.22 GBq (35–45 mCi) of [82]Rb was infused from a strontium-rubidium generator over 20–30 s with patients at rest. A similar activity was injected over 20–30 s at peak pharmacologic stress 50–60 s following initiation of regadenoson injection [17]. Blood pressure, heart rate and cardiac rhythm were recorded throughout imaging and pharmacologic testing.

Tomograms were reconstructed by OSEM (20 subsets; 2 iterations; z-axis filter = "standard"; post-filter = 2.57 mm FWHM). Image reconstruction incorporated corrections for scattered and random events and CT attenuation correction. First pass data were re-binned as: 20 3 s frames, 5 12 s

frames and 7 30 s frames. Myocardial equilibrium portions of the acquisition were re-binned as gated tomograms at 8 frames/R–R interval.

Myocardial perfusion

[82]Rb-specific normal limits were applied to equilibrium short axis images to obtain LV relative perfusion summed stress scores (SSS), summed rest scores (SRS) and summed difference scores (SDS) by an artificial intelligence-driven approach [18]. Territorial left anterior descending (LAD), left circumflex (LCX) and right coronary artery (RCA) relative perfusion scores, as well as global scores, were tabulated. Rest and stress global LV ejection fraction (EF) from gated equilibrium data were calculated [19]. The available algorithms computed only global EF's, not regional EF's.

Semi-automated software computed MBF from dynamic first-pass data [20, 21]. Quality assurance algorithms were applied to all data to preclude from subsequent analysis any cases with possible technical data acquisition problems [21]. Rest and stress MBF and MFR values were obtained for each of the three main coronary arterial territories (Fig. 1). MFR < 2.0 is considered abnormal [2], and MFR < 1.6 is a prognostic indicator for significant adverse cardiac events [3].

Each patient's three major coronary arterial territories were assigned a CFC category, derived from regional MFR and stress MBF values, following [82]Rb-PET CFC classification thresholds [22], defined as:

CFC1: Normal CFC: MFR > 2.90 and stress MBF > 2.17 ml/g/min
CFC2: Minimally reduced CFC: MFR = 2.38–2.90 and stress MBF = 1.82–2.17 ml/g/min
CFC3: Mildly reduced CFC: MFR = 1.60–2.38 and stress MBF = 1.09–1.82 ml/g/min
CFC4: Moderately reduced CFC: MFR = 1.27–1.60 and stress MBF = 0.83–1.09 ml/g/min
CFC5: Severely reduced CFC: MFR ≤ 1.27 and stress MBF ≤ 0.83 ml/g/min

These same criteria were applied to global MFR and global stress MBF to form a global measure of CFC for each patient. Because cases with CFC ≥ 4 correspond to MFR ≤ 1.6, a marker of a reduced prognosis [3, 23], we defined "abnormal CFC" as CFC ≥ 4.

LV function

The degree of abnormality of rest and stress equilibrium data regional LV wall thickening (WT) was quantified on a 5-point scale [24]. A regional composite WT value also was computed as the mean of regional rest and stress WT
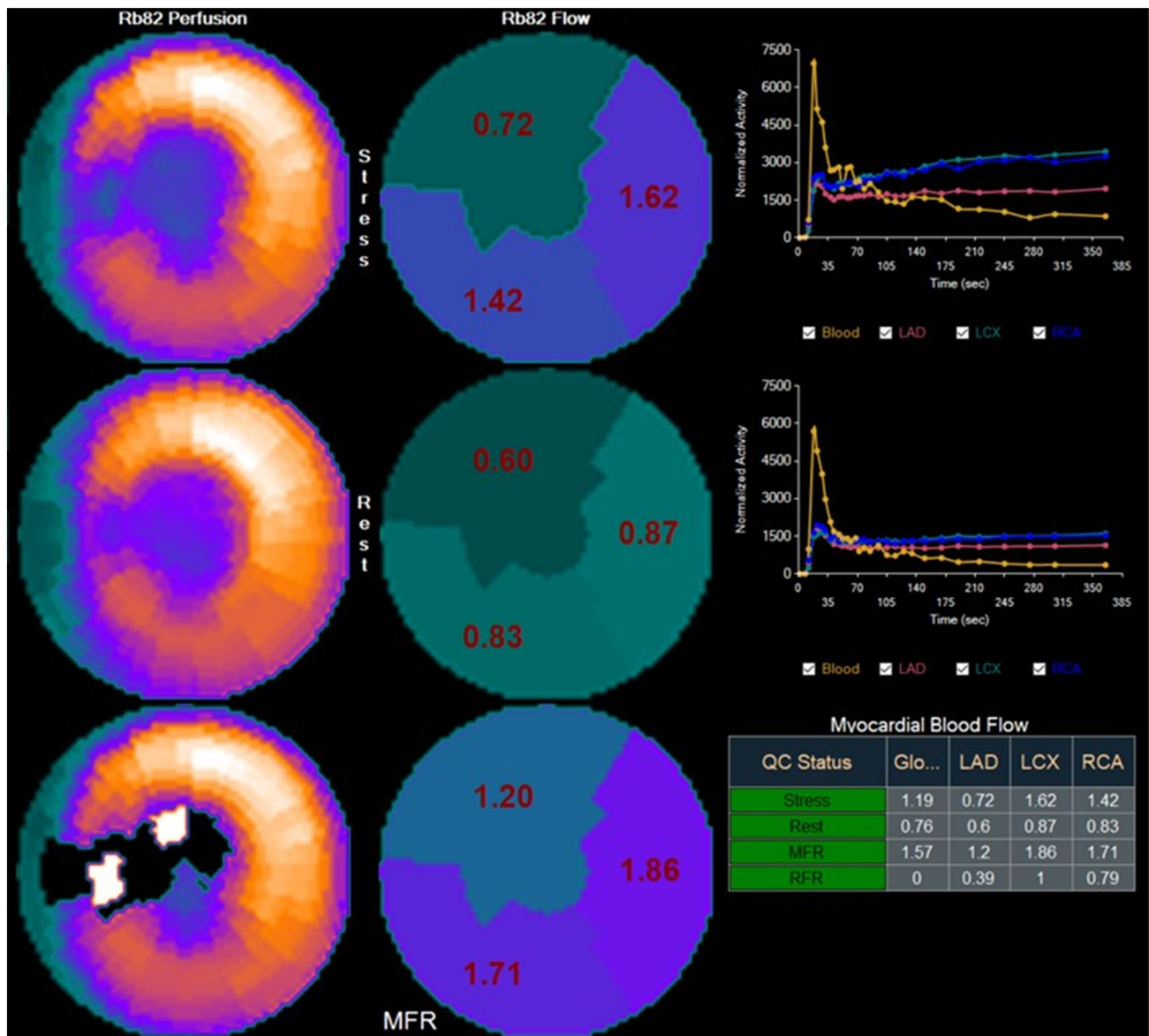
Fig. 1 Example of polar maps with territorial values of rest and stress MBF and MFR for a patient with a severe LAD stenosis

values. Global and regional rest and stress contraction phase bandwidth (BW), which quantifies the amount of the R–R interval over which 95% of systolic contractions occur, were computed from equilibrium gated tomograms (SyncTool) [25] (Fig. 2). Algorithms were written to compute regional BW within locations defined in the same way as boundaries that are routinely displayed on polar maps of relative perfusion and MBF (Fig. 1).

Angiography

Quantified x-ray contrast arteriographic measurements were performed for the subgroup of 105 patients. Coronary angiograms were acquired using standard techniques. Digitized cinematic image files were transmitted to a core lab (Boston Clinical Research Institute, BCRI, Boston, MA), where expert cardiologists quantified stenosis by planimetry using "PlusPlus" software (Sanders Data Systems, Palo Alto, CA). Cardiologists had no knowledge of PET imaging results or other clinical information. % stenosis was measured for each artery judged to have at least a 20% stenosis. Lesions in vessels < 2.0 mm in diameter were not assessed unless the lesion was in a vascular segment that was the primary conduit of circulation for any myocardial wall/segment, or if the artery segments would be ≥ 2.0 mm in diameter if fully perfused. Stenosis measurements were entered into a spreadsheet for every lesion that was scored. Each lesion was assigned to one of three major arterial territories. The maximum
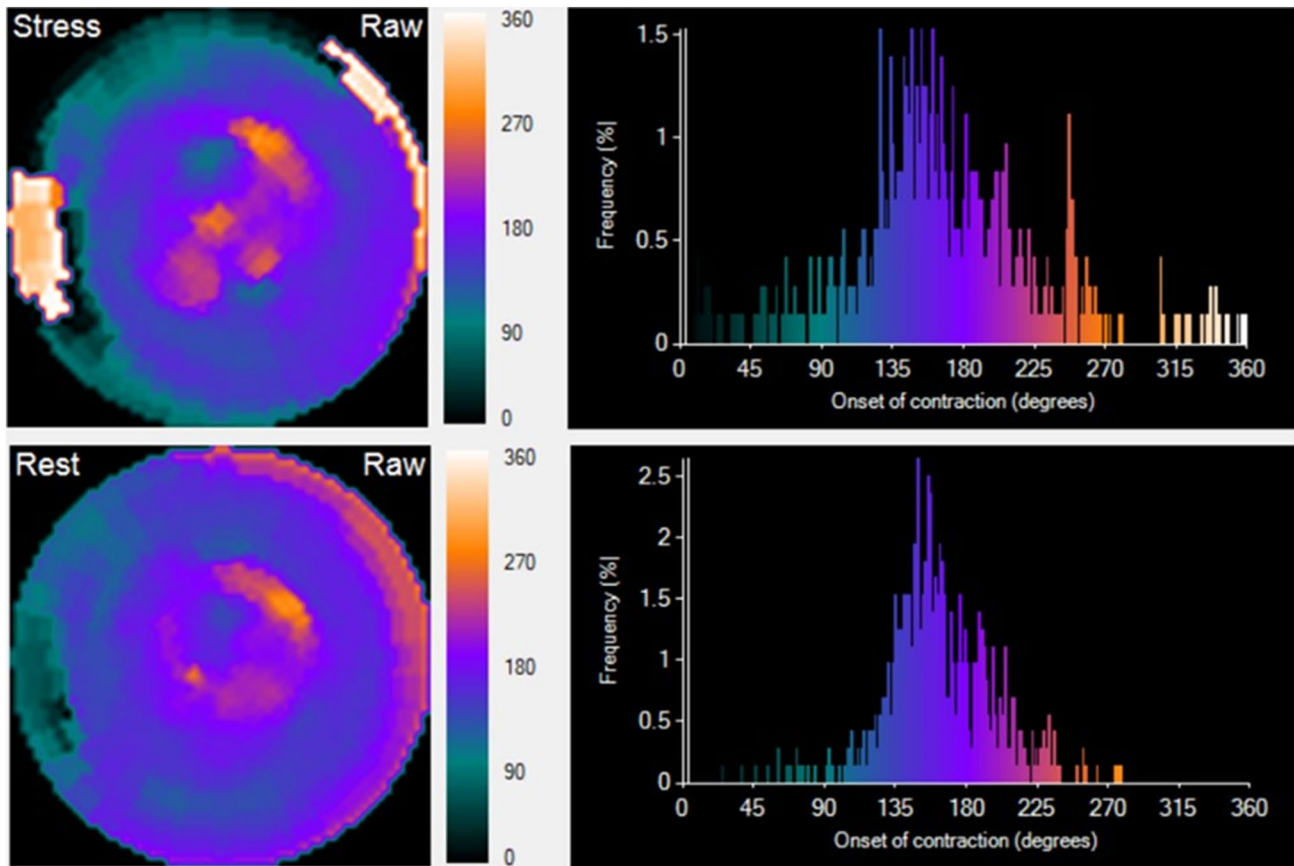
Fig. 2 For the same example as Fig. 1, BW polar maps and phase histograms for rest and stress

stenosis value was assigned to each arterial territory. For any territory for which no lesion was discerned, a value of 0% stenosis was entered into the spreadsheet.

Statistical analyses

Analyses were performed using "MedCalc" statistical software [26]. Values are reported as means ± one standard deviation. Normality of distributions were assessed by the χ^2 test. ANOVA assessed whether there were differences among variables by CFC class, adjusted by Bonferroni corrections. The unpaired or paired t-test, or Mann–Whitney or Wilcoxon test, compared values between groups of variables, as appropriate. χ^2 analysis of proportions compared ratios. Univariate logistic regression assessed ability of variables to discriminate between normal-to-mildly reduced CFC cases (CFC1-CFC3) from moderately-to-severely reduced CFC cases (CFC ≥ 4). Multivariate logistic regression analysis was used to form predictive indices, component parameters of which were retained only if association probability of each was < 0.05. ROC analysis determined accuracy (area under curve, AUC), sensitivity and specificity of parameters to identify CFC ≥ 4 cases, with thresholds of discrimination

identified as the Youden index. Significance of differences in ROC AUC values of simultaneously analyzed parameters was assessed [27]. Rank correlation determined strength of association between continuous variables and CFC categories, for which Spearman's correlation coefficients (ρ) were generated. For all tests, probability (p) < 0.05 was defined as statistically significant, or as adjusted by Bonferroni corrections for comparisons among multiple categories.

Results

Predictors of global CFC

Among 231 patients, all descriptors in Table 1 but ΔWT and ΔBW were significant predictors (overall model fit p < 0.05) of global CFC ≥ 4 by univariate logistic regression. By multivariate logistic regression analysis, only stress EF, SSS and stress BW retained significance. These parameters were combined to form a

Table 1 ROC results for parameters identifying patients with moderately-to-severely reduced global CFC

Regional parameter	ROC threshold	ROC AUC	Sensitivity (N=40)	Specificity (N=191)	Global CFC≥4 (N=40)	Global CFC<4 (N=191)
SRS	>2	75±4%*	80%	70%	9.2±8.7†	3.2±5.6
SSS	>4	80±3%	88%	62%	15.6±11.2†	6.1±8.8
SDS	>1	72±5%*	83%	62%	6.4±6.3†	3.0±5.5
Rest EF	<54%	79±4%	90%	62%	40±16%†	57±16%
Stress EF	<57%	82±3%	88%	65%	39±17%†	61±17%
ΔEF	<−4%	63±5%*	43%*	82%*	−1±8%†	+4±8%
Rest WT	>1	77±4%	89%	63%	6.0±3.8†	2.6±4.0
Stress WT	>0	78±5%	81%	67%	5.9±4.4†	1.8±3.4
ΔWT	>0	53±7%*	30%*	93%*	0.0±2.7	−1.0±2.3
Rest BW	>102°	78±4%	58%*	71%	166±70°†	94±67°
Stress BW	>75°	80±3%	88%	64%	159±80°†	85±68°
ΔBW	>−48°	51±6%*	63%*	15%*	−7±65°	−10±48°
Global index	>0.8	84±3%	88%	71%	2.0±1.3†	0.4±1.1†

EF ejection fraction

*p<0.05 statistically different from Global Index, †p<0.05 for global CFC≥4 versus global CFC<4

$$\text{Global Index} = 3.025 - (0.050 \times \text{stress EF}) + (0.051 \times \text{global SSS})$$
$$+ (0.001 \times \text{global stress BW}) \tag{1}$$

which had the highest logistic regression association with global CFC≥4 (χ^2=51.1, p<0.0001; odds ratio=2.72), and the highest ROC AUC=84±3% (Table 1).

The parameter most strongly associated with increasing severity of global CFC (highest ANOVA F-ratio=64.0, p<0.001) was the Global Index, for which highest rank correlation of ρ=0. 56 also was found (Table 2). By ANOVA, among all parameters, the Global Index most significantly distinguished cases of global CFC1-2 from CFC3, and CFC3 from CFC4 and CFC5 (Fig. 3).

Table 2 ANOVA results of LV global perfusion and function parameters for patients classified by global CFC categories

Global parameter	Global CFC1 (N=79)	Global CFC2 (N=33)	Global CFC3 (N=79)	Global CFC4 (N=26)	Global CFC5 (N=14)	Spearman's ρ
SRS	2.3±3.9	1.8±4.1	4.6±6.9	8.7±8.2*†	8.5±8.3*†	0.30**
SSS	4.5±7.2	3.3±6.2	9.0±10.4	15.1±10.7*†	15.4±12.5*†	0.39**
SDS	2.2±4.7	1.5±3.3	4.3±6.5	6.4±5.8*†	6.9±7.4*†	0.30**
Rest EF	62±14%	60±14%	51±17%*	41±17*†	37±19%*†	0.47
Stress EF	67±14%	65±13%	53±17%*†	42±17†§	35±18%*†§‡	0.53
ΔEF	4.4±8.2%	4.7±8.1%	2.2±8.6%	0.4±9.2%	−2.2±7.0%	0.19**
Rest WT	1.8±3.3	2.2±4.3	3.3±4.4	5.6±4.0*	6.5±3.5*	0.40**
Stress WT	1.0±2.0	1.9±4.0	2.4±3.9	5.1±4.4*	7.2±4.2*†§	0.43
ΔWT	−0.8±1.8	−0.3±1.7	−0.8±2.9	−0.5±2.3	0.7±3.3	0.05**
Rest BW	76±57°	85±64°	117±72°*	158±73°*†	179±66°*†	0.23**
Stress BW	69±61°	67±34°	110±79°*	144±84°*†	189±71°*†§	0.47
ΔBW	−7±38°	−18±44°	−8±57°	−13±71°	9±55°	0.05**
Global index	0.0±1.0	0.0±0.8	1.0±1.2*†	1.9±1.3*†§	2.3±1.3*†§	0.56

CFC coronary flow capacity, *CFC1* normal CFC, *CFC2* minimally reduced, *CFC3* mildly reduced, *CFC4* moderately reduced, *CFC5* severely reduced

*p<0.05 versus CFC1, †p<0.05 versus CFC2, §p<0.05 versus CFC3, ‡p<0.05 versus CFC4, **p<0.05 versus Global Index Spearman's ρ
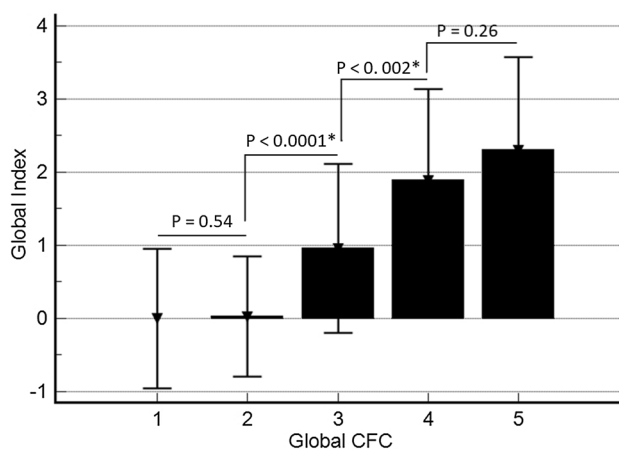
Fig. 3 Global index versus global CFC

Descriptors of regional CFC

Univariate logistic regression analyses identified parameters associated with CFC class of worsening severity in individual vascular territories. These analyses showed SSS and BW were significant predictors of CFC class, and that composite BW value had higher χ^2 association and ROC AUC than either regional rest or stress BW separately. Consequently, composite regional BW values were used for further computations. Similarly, composite WT had higher χ^2 association and ROC AUC than either regional rest or stress WT separately, so that a composite value was also used for WT.

An index combining SSS and BW, termed the

$$\text{Regional Index} = -4.94 + (0.229 \times \text{regional SSS}) \\ + (0.019 \times \text{regional stress BW}) \tag{2}$$

had highest association with regional CFC ≥ 4 ($\chi^2 = 98.1$, $p < 0.0001$; odds ratio $= 2.72$). By ROC analysis, the Regional Index had a higher accuracy ($88 \pm 3\%$) for detecting CFC ≥ 4 than any of the other regional parameters, exceeding that for quantified coronary stenoses ($88 \pm 3\%$ versus $68 \pm 4\%$, $p < 0.0001$) (Table 3).

The parameter most strongly associated with increasing severity of regional CFC (highest ANOVA F-ratio $= 53.5$, $p < 0.001$) was the Regional Index, for which highest rank correlation of $\rho = 0.58$ also was found (Table 4).

Table 3 ROC results for parameters identifying arterial territories with moderately-to-severely reduced CFC in the subgroup of 105 patients with angiography

Regional parameter	ROC threshold	ROC AUC	Sensitivity (N=60)	Specificity (N=255)	CFC≥4 (N=60)	CFC<4 (N=255)
Stenosis	>72%	68±4%*	48%*	87%*	54±43%†	26±35%
SRS	>0	77±3%*	82%	62%*	4.0±3.5†	1.4±2.4
SSS	>4	80±3%*	73%*	76%	8.0±5.4†	2.4±3.8
SDS	>2	73±4%*	57%*	87%*	4.0±4.1†	1.1±2.4
Composite WT	>0	76±3%*	73%	73%	4.8±4.8†	1.2±2.8
Composite BW	>167°	76±4%*	73%*	83%*	172±59°†	113±55°
Regional index	>1.2	88±3%	90%	74%	2.8±1.5†	0.5±1.3

*$p < 0.05$ statistically different from Regional Index, †$p < 0.05$ for regional CFC≥ 4 versus regional CFC< 4

Table 4 ANOVA results of LV regional perfusion and function parameters for arteries classified by arterial territory CFC category in the subgroup of 105 patients with angiography

Regional parameter	Regional CFC1 (N=100)	Regional CFC2 (N=49)	Regional CFC3 (N=106)	Regional CFC4 (N=45)	Regional CFC5 (N=15)	Spearman's ρ
% stenosis	20±32%	30±34%	29±38%	45±43%*	79±33%*†§‡	0.27**
SRS	0.8±1.3	1.5±2.9	1.9±2.7	3.8±3.5*†§	4.6±3.6*†§	0.37**
SSS	1.3±2.1	2.5±3.9	3.6±4.5*	7.4±5.2*†§	10.0±5.3*†§	0.46**
SDS	0.5±1.2	1.0±2.0	1.7±3.1*	3.6±4.1*†§	5.4±3.7*†§	0.30**
Composite WT	0.7±1.9	1.4±3.5	1.7±3.2	3.9±3.9*†§	7.5±6.2*†§‡	0.46**
Composite BW	102±47°	97±50°	131±59°*†	163±64°*†§	200±27°*†§	0.39**
Regional index	0.0±1.0	0.2±1.4	1.1±1.3*†	2.5±1.5*†§	3.7±1.3*†§‡	0.58

*$p < 0.05$ versus CFC1, †$p < 0.05$ versus CFC2, §$p < 0.05$ versus CFC3, ‡$p < 0.05$ versus CFC4, **$p < 0.05$ versus BW+SSS Spearman's ρ
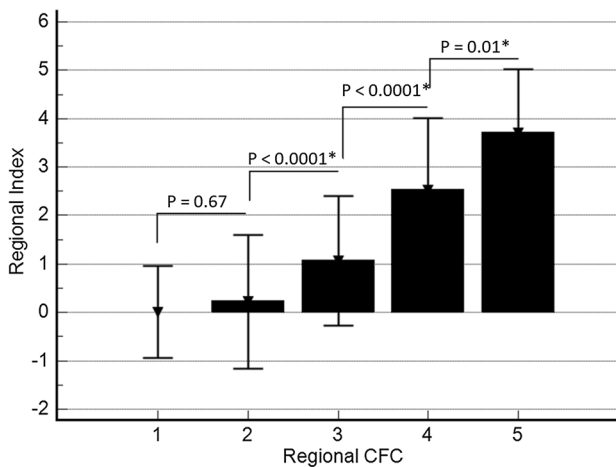
Fig. 4 Regional index versus regional CFC

Fig. 5 Percentage of arteries with abnormally elevated Regional Index values (> 1.4) versus regional CFC
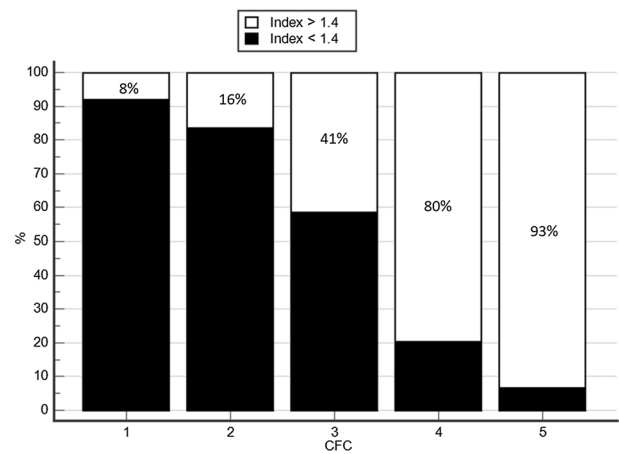
By ANOVA, the Regional Index distinguished cases of regional CFC1-2 from CFC3, CFC3 from CFC4, and CFC4 from CFC5 (Table 4; Fig. 4). Angiographic % stenosis became progressively more severe with increasing CFC category, but its rank correlation was not as strong as for the Regional Index ($\rho = 0.27$ versus $\rho = 0.58$, $p < 0.0001$) (Table 4).

Defining limits of the regional index in normal coronary arteries

Among the angiography subgroup, there were 171 arteries with 0–19% stenosis, 75 arteries with 20–69% stenosis and 69 arteries with ≥ 70% stenosis. ROC analysis indicated that a value of the Regional Index > 1.4 best separated arteries with 0–20% stenosis from all other arteries with greater degree of anatomic obstruction. A regional Index of > 1.4 can thus be used as a threshold value defining upper limits of heterogeneous perfusion and asynchrony seen in angiographically non-obstructed arteries. Arterial territories with values of the Regional index above this threshold demonstrate perfusion and LV dysfunction abnormalities characteristic of ischemia. Using a threshold of Regional Index > 1.4, percentages of arterial territories with elevated Regional Index values rose progressively with increasing CFC, as 8%, 16%, 41%, 80% and 93% from CFC1 to CFC5, respectively (Fig. 5).

Discussion

Our study documents that globally, relative perfusion, wall thickening, EF and asynchrony all worsen progressively in concert with CFC (Table 2). Even for patients with only mildly reduced CFC (CFC3), where values for MFR (1.6–2.38)

overlap "normal" as defined by societal guidelines, there were significant reductions in rest and stress EF, worsening BW and increased Global Index. Analogous patterns were seen when CFC of separate territories were analyzed (Table 4): individual vascular territories with even mildly abnormal CFC showed small but significant worsening of relative perfusion and BW. The upper limit of the Regional Index in non-obstructed coronary arteries was 1.4. Few arterial territories in CFC1 or CFC2 categories had a Regional Index above this level, but for CFC3 (with only mildly reduced MBF) up to 40% of territories had an abnormal Regional Index, suggesting early relative perfusion abnormality and ischemic LV dysfunction/asynchrony (Fig. 5). In moderate-to-severe CFC categories, most arteries had an abnormal Regional Index.

CFC in predicting cardiac risk and benefits of revascularization

CFC combines stress MBF and MFR in graded categories of MBF ranging from Normal to Severely Reduced [10]. Advantages of CFC over routine analysis of MFR include its ability to incorporate variability of regional resting MBF, and its ease of translation into catheterization derived physiologic variables [28]. CFC has been used to identify patients at high risk for MACE, who would benefit from revascularization [9, 11]. Patients with even small areas of severely reduced CFC were at a heightened risk of MACE, which could be reduced 45–60% by early PCI or CABG. Vascular territories with severely reduced CFC and a perfusion defect affecting 10% of myocardium have demonstrated a 58% increase in MBF after revascularization [11]. However, arteries with less severely reduced CFC could also demonstrate improved stress MBF after re-vascularization, by as much as 40%, if perfusion defects were present, suggesting that severely reduced CFC was not always necessary for a

beneficial result. Miura et al. averaged MFR and stress MBF over an entire vascular distribution to classify a coronary artery's CFC class [12], similar to the methodology used in our study. Using ^{13}N–H_3, they compared the outcomes of 34 patients with "impaired CFC" (defined as mildly reduced CFC or worse in at least one territory) versus 103 patients with "unimpaired CFC." MACE were significantly higher (26% vs. 2%) in "impaired" versus "unimpaired" patients, and 82% of "impaired" patients had only mildly reduced CFC. Effects of revascularization on vessel-specific CFC values in 314 patients and 415 arterial territories using pre- and post-intervention has been studied with ^{15}O–H_2O PET [13], demonstrating significant improvements in CFR, stress MBF and CFC category for all CFC classes. Greater increase in flow values were seen with worse CFC, and prognosis was associated with degree of CFC improvement. Patients with coronaries having even mildly to moderately reduced CFC have been reported to have excess MACE by a factor of 2.1–7.1 [28]. These findings support the concept that both mild and more severe impairment of CFC have prognostic import, and that re-vascularization may improve MBF and outcomes.

CFC in relation to current data

In our study we established an index combining stress perfusion defect size (SSS) and stress-induced LV asynchrony (stress BW) that closely parallels worsening regional MBF. As CFC class worsens, the frequency of arteries with an abnormally elevated Regional Index, and the potential to develop stress perfusion defects and ischemic LV asynchrony increases.

The Regional Index may be a useful addition to standard imaging parameters, particularly in patients in whom there is inconsistency between clinical information, MBF and/or CFC data and perfusion findings. For patients in the CFC categories < 4, an abnormal Regional Index could trigger further studies such as use of FFR to clarify a patient's coronary status. On occasion, technical difficulties can interfere with the injection of a radioactive bolus, so that accurate assessment of MBF and CFC may be compromised. One study reported that 7% of patients had technical problems with data acquisitions, despite all injections having been perceived as successfully delivered at the time of data acquisition [21]. Because SSS is measured from ungated equilibrium data, and EF and asynchrony measured from gated equilibrium data, not first-pass images, these measurements may not be affected by suboptimal delivery of an injection. In that setting, an abnormal Regional Index could provide an indication as to whether an arterial stenosis can cause ischemic LV dysfunction/asynchrony in response to stress, and should be evaluated further.

Limitations

Ours was a high-risk cohort of patients. All of the patients referred for PET scans had known or suspected CAD. Even though a substantial number of our patients had normal CFC (CFC category 1), we would have had a more complete picture of the clinical utility of the Global Index and Regional Index values if we also had a group of normal subjects with no symptoms suggestive of CAD. We also were hampered from exploring some potentially important clinical questions by our sample size being inadequate to test whether individual risk factors (MI, pre-CABG, etc.) were significantly associated with abnormal indices.

We also would have liked to have some information regarding the utility of these indices for predicting the success of ravasularization. We have no such information for the patients studied in the investigation, and future prospective studies would be required to obtain such information.

Conclusion

Arteries with abnormal CFC derived from absolute myocardial blood flow measurements are accurately identified by composite parameters combining regionally aberrant relative perfusion patterns and asynchrony.

Declarations

References

1. Mc Ardle BA, Dowsley TF, deKemp RA, Wells GA, Beanlands RS (2012) Does rubidium-82 PET have superior accuracy to spect perfusion imaging for the diagnosis of obstructive coronary disease? A systematic review and meta-analysis. J Am Coll Cardiol 60:1828–1837

2. Murthy VL, Bateman TM, Beanlands RS, Berman DS, Borges-Netok S, Chareonthaitawee P et al (2018) Clinical quantification of myocardial blood flow using PET: joint position paper of the SNMMI cardiovascular council and the ASNC. J Nucl Cardiol 25:269–297

3. Taqueti VR, Hachamovitch R, Murthy VL, Naya M, Foster CR, Hainer J et al (2015) Global coronary flow reserve is associated with adverse cardiovascular events independently of luminal angiographic severity and modifies the effect of early revascularization. Circulation 131:19–27

4. Gould KL, Johnson NP, Bateman TM, Beanlands RS, Bengel FM, Bober R et al (2013) Anatomic versus physiologic assessment of coronary artery disease. Role of coronary flow reserve, fractional flow reserve, and positron emission tomography imaging in revascularization decision-making. J Am Coll Cardiol 62(18):1639–1653

5. Ali ZA, Horst J, Gaba P, Shaw LJ, Bangalore S, Hochman JS et al (2021) Standardizing the definition and analysis methodology for complete coronary artery revascularization. J Am Heart Assoc 10:e020110. https://doi.org/10.1161/JAHA.120.020110

6. Ficaro EP, Lee BC, Kritzman JN, Corbett JR (2007) Corridor4DM: the Michigan method for quantitative nuclear cardiology. J Nucl Cardiol 14:455–465

7. Taqueti VR, Di Carli MF (2016) Clinical significance of noninvasive coronary flow reserve assessment in patients with ischemic heart disease. Curr Opin Cardiol 31(6):662–669

8. Di Carli MF, Hachamovitch R (2019) Quantitative coronary flow capacity for risk stratification and clinical decision making: Is it ready for prime time? J Nucl Med 60(3):407–409

9. Gould KL, Johnson NP, Roby A, Nguyen Tung T, Kirkeeide RL, Haynie M et al (2019) Regional artery-specific thresholds of quantitative myocardial perfusion by PET associated with reduced MI and death after revascularization in stable CAD. J Nucl Med 60(3):410–417

10. Johnson NP, Gould KL (2012) Integrating noninvasive absolute flow, coronary flow reserve, and ischemic thresholds into a comprehensive map of physiological severity. J Am Coll Cardiol Img 5:430–440

11. Bober RM, Milani RV, Oktay AA, Javed F, Polin NM, Morin DP (2019) The impact of revascularization on myocardial blood flow as assessed by positron emission tomography. Eur J Nucl Med Mol Imaging 46(6):1226–1239

12. Miura S, Naya M, Kumamaru H, Ando A, Miyazaki C, Yamashita T (2022) Prognostic value of modified coronary flow capacity by ^{13}N-ammonia myocardial perfusion positron emission tomography in patients without obstructive coronary arteries. J Cardiol 79(2):247–256. https://doi.org/10.1016/j.jjcc.2021.09.001

13. de Winter RW, Jukema RA, van Diemen PA, Schumacher SP, Driessen RS, Stuijfzand WJ et al (2021) The impact of coronary revascularization on vessel-specific coronary flow capacity and longterm outcomes: a serial [^{15}O]H$_2$O positron emission tomography perfusion imaging study. Euro Heart J Cardiovasc Imaging 00:1–10. https://doi.org/10.1093/ehjci/jeab263

14. Van Tosh A, Votaw JR, Cooke CD, Cao JJ, Palestro CJ, Nichols KJ (2021) Early onset of left ventricular regional asynchrony in arteries with sub-clinical stenosis. J Nucl Card 28:1040–1050. https://doi.org/10.1007/s12350-020-02251-9

15. Dilsizian V, Bacharach SL, Beanlands RS, Bergmann SR, Delbeke D, Dorbala S et al (2016) ASNC imaging guidelines/SNMMI procedure standard for positron emission tomography (PET) nuclear cardiology procedures. J Nucl Cardiol 23:1187–1226

16. Bravo PE, Pozios I, Pinheiro A, Merrill J, Tsui BM, Wahl RL et al (2012) Comparison and effectiveness of regadenoson versus dipyridamole on stress electrocardiographic changes during positron emission tomography evaluation of patients with hypertrophic cardiomyopathy. Am J Cardiol 110:1033–1039

17. Johnson NP, Gould KL (2015) Regadenoson versus dipyridamole hyperemia for cardiac PET imaging. J Am Coll Cardiol Img 8:438–447

18. Garcia EV, Klein JL, Moncayo V, Cooke CD, Del'Aune C, Folks R et al (2018) Diagnostic performance of an artificial intelligence-driven cardiac-structured reporting system for myocardial perfusion SPECT imaging. J Nucl Cardiol. https://doi.org/10.1007/s12350-018-1432-3

19. Faber TL, Cooke DC, Folks RD, Vansant JP, Nichols KJ, DePuey EG et al (1999) Left ventricular function from gated SPECT perfusion images: an integrated method. J Nucl Med 40:650–659

20. Votaw JR, Packard RRS (2017) Technical aspects of acquiring and measuring myocardial blood flow: method, technique, and QA. J Nucl Cardiol. https://doi.org/10.1007/s12350-017-1049-y

21. Van Tosh A, Votaw JR, Cooke CD, Cao JJ, Palestro CJ, Nichols KJ (2021) Clinical implications of compromised ^{82}Rb PET data acquisition. J Nucl Card 28(4):1409–1412. https://doi.org/10.1007/s12350-021-02774-9[doi]

22. Gould KL, Kitkungvan D, Johnson NP, Nguyen T, Kirkeeide R, Bui L et al (2021) Mortality prediction by quantitative PET perfusion expressed as coronary flow capacity with and without revascularization. JACC Cardiovasc Imaging 14(5):1020–1034

23. Murthy VL, Naya M, Foster CR, Hainer J, Gaber M, Di Carli G et al (2011) Improved cardiac risk assessment with noninvasive measures of coronary flow reserve. Circulation 124:2215–2224

24. Cooke CD, Garcia EV, Cullom SJ, Faber TL, Pettigrew RI (1994) Determining the accuracy of calculating systolic wall thickening using a fast Fourier transform approximation: a simulation study based on canine and patient data. J Nucl Med 35(7):1185–1192

25. Chen J, Garcia EV, Folks RD, Cooke CD, Faber TL, Tauxe EL et al (2005) Onset of left ventricular mechanical contraction as determined by phase analysis of ECG-gated myocardial Perfusion SPECT imaging: development of a diagnostic tool for assessment of cardiac mechanical dyssynchrony. J Nucl Cardiol 12:68–95

26. MedCalc Statistical Software version 20.110 (MedCalc Software Ltd, Ostend, Belgium; https://www.medcalc.org; 2022)

27. Hanley JA, McNeil BJ (1983) A method of comparing the areas under receiver operating characteristic curves derived from the same cases. Radiology 148:839–843

28. van de Hoef TP, Echavarría-Pinto M, van Lavieren MA et al (2015) Diagnostic and prognostic implications of coronary flow capacity: a comprehensive cross-modality physiological concept in ischemic heart disease. ACC Cardiovasc Interv 8:1670–1680